



# The sensitive detection of ATP and ADA based on turn-on fluorescent copper/silver nanoclusters

Baozhu Zhang<sup>1,2</sup> · Chunying Wei<sup>1</sup>

Received: 20 November 2019 / Revised: 27 January 2020 / Accepted: 31 January 2020 / Published online: 10 February 2020  
© Springer-Verlag GmbH Germany, part of Springer Nature 2020

## Abstract

A simple turn-on fluorescence strategy is proposed for the detection of ATP based on DNA-stabilized copper/silver nanoclusters (DNA-Cu/Ag NCs). The fluorescence intensity of DNA-Cu/Ag NCs increases significantly in the presence of ATP, because the specific interaction between ATP and its aptamer causes two darkish Cu/Ag NCs to be situated at the 5' and 3' termini close to each other. A limit of detection (LOD) of 7.0  $\mu\text{M}$  is found, in a linear range of 2–18 mM, and the proposed sensor is simple, sensitive, and selective. Additionally, the DNA-Cu/Ag NCs/ATP system is further developed into a sensor for ADA detection and demonstrates a linear response to ADA from 5 to 50 U/L with a LOD of 5 U/L. The proposed method is also shown to be successful in detecting ATP and ADA in a solution of fetal bovine serum.

**Keywords** DNA-Cu/Ag NCs · Aptamer · ATP · ADA · Fluorescence

## Introduction

Metal nanoclusters (NCs), which are composed of several to hundreds of metal atoms with diameters less than 2 nm, have been widely utilized to construct fluorescent sensors for detecting various biological or chemical analytes, as an emerging alternative to organic fluorophores [1–3]. In particular, DNA-templated metal NCs have been used for the detection of different analytes, including DNA, cells, biomolecules, anions, and metal ions [4–9], as they possess various advantages over quantum dots or organic fluorophores, including lower toxicity, large Stokes shift, biocompatibility, good photostability, strong fluorescence, ease of preparation, and tunable fluorescence wavelengths from blue to near-infrared emission by altering the strand lengths or base sequences of the DNA oligonucleotides [10–14].

The representative examples belong to ‘light-up’ sensors: for instance, when a guanine-rich DNA sequence gets close to non-emissive metal NCs scaffolded by DNA in colorimetric biosensors, they are converted to bright emitters [2, 15–17]. Other systems of ‘light-off’ types depend on the interaction of the fluorescent DNA-templated metal NCs with certain quenchers, for example, thiol-containing chemicals and sulfide ions, which have been developed into novel sensors for the detection of thiol-containing chemicals and sulfide ions utilizing the quenching phenomenon [18, 19].

Adenosine 5'-triphosphate (ATP), as a typical energy molecule, has attracted increasing attention in recent years; it plays a key role as a fundamental component in protein metabolism and cell energy generation [20, 21] and as an endogenous modulator in regulating various physiological processes in diverse tissues and organs [22, 23]. Additionally, researchers have demonstrated that adenosine may serve as a potential biomarker for cancer detection [24]. Hence, a number of methods have been developed for ATP detection, including capillary electrophoresis (CE) [25], radioimmunoassay [26], high-performance liquid chromatography (HPLC) [27], and aptamer-based methods [28–30]. However, they inevitably suffer from modified fluorescent probes and/or complicated sample preparation procedures. Therefore, in order to serve the needs of biochemical research and clinical diagnosis, a far more accurate and convenient method for detecting ATP is needed.

**Electronic supplementary material** The online version of this article (<https://doi.org/10.1007/s00216-020-02476-0>) contains supplementary material, which is available to authorized users.

✉ Chunying Wei  
weichuny@sxu.edu.cn

<sup>1</sup> Key Laboratory of Chemical Biology and Molecular Engineering of Ministry of Education, Institute of Molecular Science, Shanxi University, Taiyuan 030006, Shanxi, China

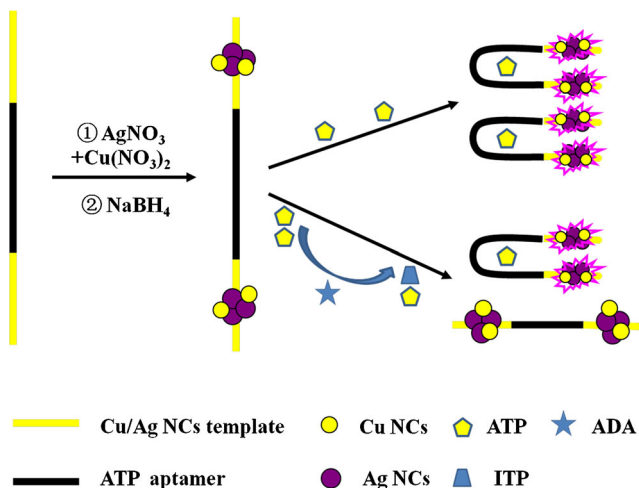
<sup>2</sup> College of Chemistry and Chemical Engineering, Jinzhong University, Yuci 030619, Shanxi, China

It is reported that the fluorescence of two darkish DNA-Ag NCs can increase significantly when they are close to each other by their complementary linkers [31]. Motivated by this idea, a turn-on fluorescence method was constructed based on DNA-templated copper/silver nanoclusters (DNA-Cu/Ag NCs) for the detection of ATP. As shown in Scheme 1, the DNA template is composed of the Cu/Ag NCs-nucleation segment at the two termini and the ATP aptamer in the middle of the DNA template. The system takes advantage of the fact that the two darkish DNA-Cu/Ag NCs become bright emitters when they are close to each other, due to the conversion of the aptamer conformation in the presence of ATP. Therefore, it enables the turn-on, sensitive, selective, and convenient detection of ATP. In addition, adenosine deaminase (ADA) is an important enzyme; it exists in all human tissues, particularly in the lymphoid system, and it can catalyze the conversion of adenosine to inosine by removing an amino group [32]. Therefore, the DNA-Cu/Ag NCs/ATP system is developed as a method for detecting ADA activity.

## Experimental

### Reagents and apparatus

Oligonucleotides, ATP, ADA, cytidine 5'-triphosphate (CTP), uridine 5'-triphosphate (UTP), and guanosine 5'-triphosphate (GTP) used in this work were purchased from Sangon Biotechnology Inc. (Shanghai, China), and the names and sequences of DNA oligonucleotides are listed in Table S1 in the Electronic Supplementary Material (ESM). Fetal bovine serum was obtained from Beijing Solarbio Biotechnology Co., Ltd. (China).  $\text{Cu}(\text{NO}_3)_2$ ,  $\text{AgNO}_3$  (99.8%), and  $\text{NaBH}_4$  (98%) were provided by Aladdin Bio-chem technology Co., Ltd. (Shanghai, China). All chemical reagents were analytical grade and were used as received without further purification. Phosphate buffer



**Scheme 1** Schematic illustration of the method for ATP and ADA detection based on DNA-Cu/Ag NCs.

solution (PBS, 20 mM, pH 7.0) was used in all of the experiments. Milli-Q water (18.2 M $\Omega$  cm) was utilized in all solutions.

UV-vis spectra were acquired at ambient temperature on a Cary 50 Bio spectrophotometer (Varian Inc., CA, USA). Fluorescence spectra measurements were obtained on a Hitachi F-4600 fluorescence spectrophotometer at ambient temperature, and the excitation and emission slit widths were 5.0 nm and 10 nm, respectively. The average size and morphology of the DNA-Cu/Ag NCs were determined using a JEOL JEM-2100 transmission electron microscope with 200-kV acceleration voltage. Time-resolved fluorescence measurements were recorded on an FL920 fluorescence lifetime spectrometer (Edinburgh Instruments, Livingston, UK) operating in time-correlated single-photon counting (TCSPC) mode using a semiconductor laser (405 nm) as the excitation source. Commercial software by Edinburgh Instruments was used for data analyses. When  $\sum_{i=1}^n A_i = 1$ , the average excited state life-

time is expressed by the equation  $\tau_{\text{avg}} = \sum_{i=1}^n A_i \tau_i$ . The report-

ed spectrum of each sample represents the average of three scans. X-ray photoelectron spectroscopy (XPS) (ESCALAB 220i-XL, VG Scientific, UK) was performed using monochromic Al K $\alpha$  as the source at 1486.6 eV. Circular dichroism (CD) spectroscopy of BT5T5-Cu/Ag NCs (10  $\mu\text{M}$ ) without and with 10 mM ATP was carried out at room temperature on a Chirascan circular dichroism spectrometer (Applied Photophysics Ltd., Surrey, UK), and the spectrum was obtained within the range of 220–320 nm at intervals of 1 nm intervals, employing a 1-mm optical path-length quartz cell and an instrument scanning speed of 120 nm/min.

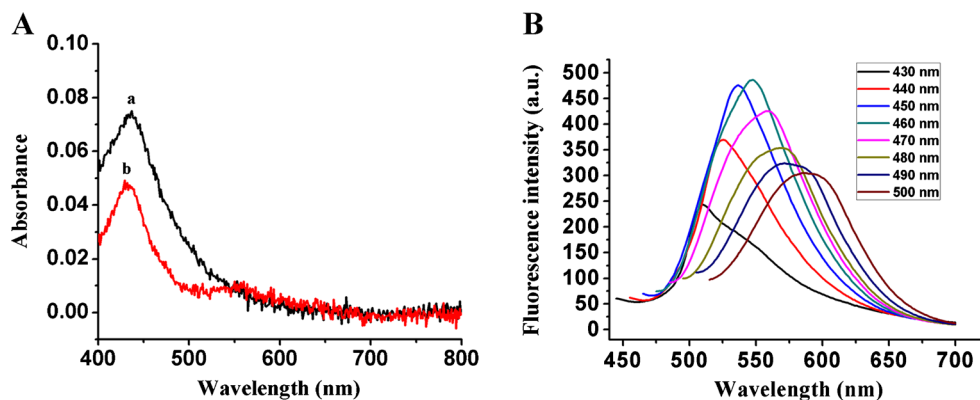
### Synthesis of DNA-Cu/Ag NCs

DNA-Cu/Ag NCs were prepared according to a previously reported method [19], with minor modifications. Briefly, DNA oligonucleotides (3.0  $\mu\text{M}$ ),  $\text{AgNO}_3$  (24  $\mu\text{M}$ ), and  $\text{Cu}(\text{NO}_3)_2$  (9.0  $\mu\text{M}$ ) were sequentially added to PBS (20 mM, pH 7.0) and mixed uniformly. After the mixture solution was kept away from light for 20 min at 4  $^\circ\text{C}$ ,  $\text{Ag}^+$  and  $\text{Cu}^{2+}$  were reduced by the freshly prepared  $\text{NaBH}_4$  (60  $\mu\text{M}$ ). The final molar ratios of DNA,  $\text{Cu}(\text{NO}_3)_2$ ,  $\text{AgNO}_3$ , and  $\text{NaBH}_4$  were 1:3:8:20. The above mixture was incubated at 4  $^\circ\text{C}$  for 1 h in the dark to obtain Cu/Ag NCs for the subsequent experiment.

### Detection of ATP and ADA

Different concentrations of ATP (0–22 mM) were added to the prepared BT5T5-Cu/Ag NCs solution, and the fluorescence spectrum of each sample was obtained at ambient temperature after incubation for 5 min. For the assay of ADA, 10 mM ATP

**Fig. 1** (A) UV-vis absorption spectra of BT5T5-Cu/Ag NCs alone (a) and with 10 mM ATP (b). (B) Fluorescence emission spectra of BT5T5-Cu/Ag NCs under different excitation wavelengths. *c* (DNA) = 3  $\mu$ M



was pre-incubated with ADA of various concentrations (0–200 U/L) in PBS (20 mM, pH 7.0) for 30 min at ambient temperature. Then the mixture was added to the prepared BT5T5-Cu/Ag NCs solution; after incubation for 5 min, the fluorescence spectra of different samples were measured. In the case of specificity of ATP, the assay procedures were performed according to those of ATP except using CTP, GTP, or UTP instead of ATP.

### Application of the proposed sensor

ATP and ADA in diluted fetal bovine serum solution were measured by employing the proposed sensing system. The samples were spiked with different concentrations of ATP and ADA and analyzed using the same method as detection of ATP and ADA.

## Results and discussion

### Optical characterization of DNA-Cu/Ag NCs

The properties of metal NCs are directly influenced by the secondary structures and base sequences of DNA templates [14, 33].

Herein, eight DNA sequences were designed based on the template BT3T3 by changing the number and types of the bases of the connecting part and the nucleation C-rich sequences, namely BT3T3, BT5T5, BT5T5(R), (L)BT5T5, BT5A5, BA3A3, BA5A5, and BG3G3 (ESM Table S1), and DNA-Cu/Ag NCs were synthesized using these templates. Among these, the aptamer of ATP (the middle part of the DNA template, *italics*) is the same, while the C-rich segments located at the 5' and/or 3' ends (**bold**) are different, and the TTT, TTTTT, AAA, AAAAA, or GGG linkers (underlined) connect the C-rich segment with the aptamer. The results of optical characterization of BT5T5-Cu/Ag NCs alone (curve a) and with 10 mM ATP (curve b) are shown in Fig. 1. Both UV-Vis absorption spectra (Fig. 1A) show an obvious peak at 430 nm that is a characteristic plasmon absorption band of nanoparticles [34, 35]. There is also a peak at about 560 nm in curve b, which can be assigned to the absorbance of the DNA-Cu/Ag NCs, indicating that the interaction of ATP with the aptamer leads to the formation of many more Cu/Ag NCs [36]. It is found that the maximum emission wavelength of BT5T5-Cu/Ag NCs depends on the excitation wavelength, and the maximum emission peak is 550 nm (Fig. 1B). For comparison, optical characterization of the BT5T5-Ag NCs with and without 10 mM ATP was also carried out (ESM Fig. S1). The UV-vis absorption spectrum (ESM Fig. S1A) of BT5T5-Ag NCs

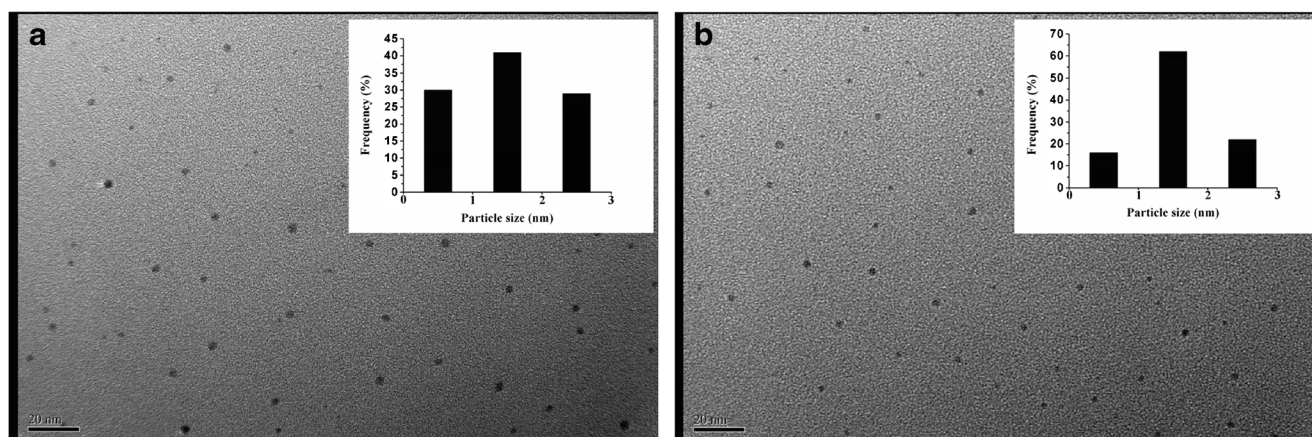


**Fig. 2** TEM images of BT5T5-Cu/Ag NCs alone (a) and with 18 mM ATP (b). The inset shows the size distribution histogram

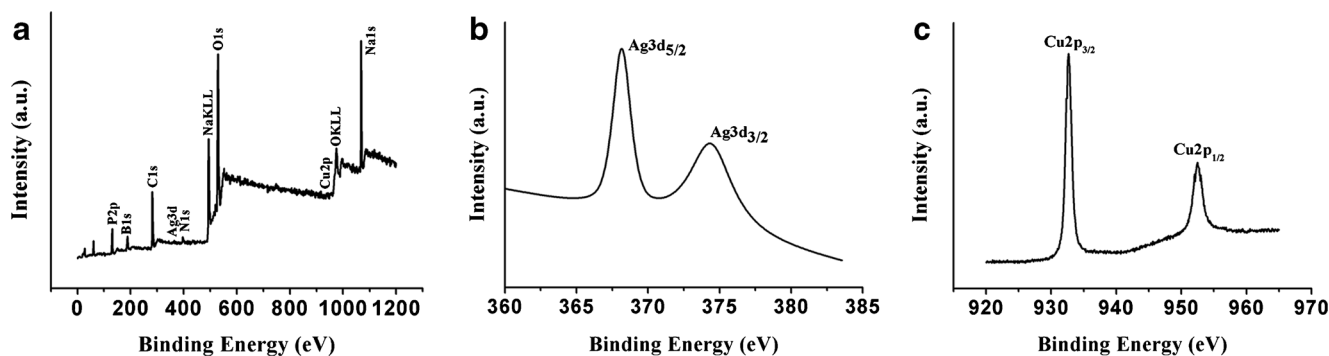


**Fig. 3** (a) XPS spectrum of BT5T5-Cu/Ag NCs. (b) Ag 3d region of XPS spectrum of BT5T5-Cu/Ag NCs. (c) Cu 2p region of XPS spectrum of BT5T5-Cu/Ag NCs

with 10 mM ATP (curve b) also shows the two peaks at about 430 and 580 nm, while only one band at 430 nm without ATP is observed (curve a). The maximum emission wavelength is 620 nm for BT5T5-Ag NCs (ESM Fig. S1B). Compared with BT5T5-Cu/Ag NCs, the emission intensity of BT5T5-Ag NCs is stronger, and the emission wavelength is longer. The UV-Vis absorption and fluorescence spectra under different excitation wavelengths of the Cu/Ag NCs based on the other seven DNA templates are shown in ESM Figs. S2 and S3, respectively. The fluorescence intensities of BT5T5-Cu/Ag NCs and BT5A5-Cu/Ag NCs are the strongest and are almost equal, while (L)BT5T5-Cu/Ag NCs and BT5T5(R)-Cu/Ag NCs display the weakest emission.

Because the stability of the probe will affect the detection performance, we measured the change in the fluorescence intensity of six DNA-Cu/Ag NCs with stronger emission against the storage time (ESM Fig. S4). The fluorescence intensity of BT5T5-Cu/Ag NCs remained stable for about 4 h, and it showed the highest stability among the six. Hence, BT5T5-Cu/Ag NCs were further characterized for good stability and strong fluorescence.

### Characteristics of BT5T5-Cu/Ag NCs

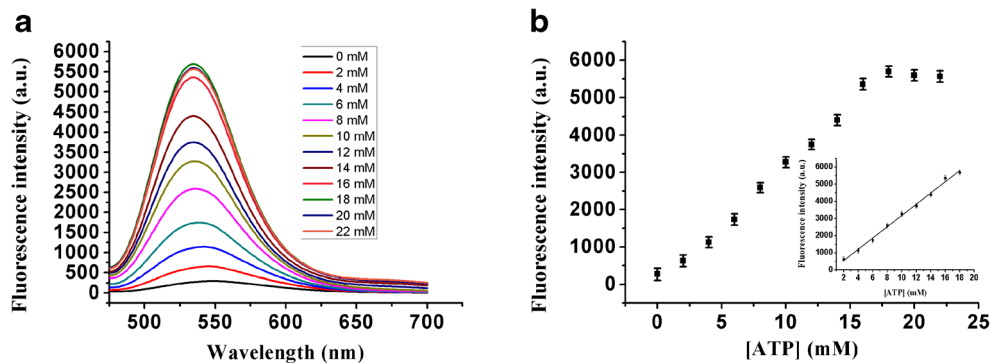
To evaluate the diameters and uniformity of BT5T5-Cu/Ag NCs, TEM images of BT5T5-Cu/Ag NCs alone and with 18 mM ATP were measured. As shown in Fig. 2a and b,

BT5T5-Cu/Ag NCs appear to be a uniformly distributed, and the average size is about 2 nm (inset of Fig. 2a and b), which meets the requirement that the core size of metal NCs is below 2.0 nm [37]. The number of BT5T5-Cu/Ag NCs with ATP with a diameter of 1–2 nm is much greater than that of BT5T5-Cu/Ag NCs alone, which can be attributed to the fact that ATP not only disperses Cu/Ag NCs but also stabilizes them [36].

CD spectra of BT5T5 DNA and BT5T5-Cu/Ag NCs were also recorded to observe the conformational change in DNA upon formation of the NCs. As indicated in ESM Fig. S5, a negative band and a broad positive band centered at 240 and 270 nm, respectively, are present in the CD spectrum of BT5T5 (curve a), while the CD spectrum of BT5T5-Cu/Ag NCs (curve b) is redshifted about 10 nm, and the intensity also weakens due to the formation of Cu/Ag NCs at the nucleation segment of the DNA template. The results indicate that the conformation of DNA is changed slightly by Cu/Ag NCs.

XPS was further performed to examine the existence of various elements and the valence state of the Ag and Cu element in the BT5T5-Cu/Ag NCs. Figure 3a confirms the presence of Cu, Ag, Na, P, O, N, C, and B. The content of Ag and Cu in Cu/Ag NCs was determined by calculating the peak areas of the elements, and revealed values of 1.13% and 2.04%, respectively. In the expanded spectrum of Ag 3d (Fig. 3b), the binding energy values at 368.15 eV and 374.3 eV belong to Ag 3d<sub>5/2</sub> and Ag 3d<sub>3/2</sub>, respectively, and

**Fig. 4** Fluorescence spectra of BT5T5-Cu/Ag NCs ( $\lambda_{\text{ex}} = 460$  nm) (a) with the addition of ATP in different concentrations. Fluorescence intensity changes in BT5T5-Cu/Ag NCs (b) with change in ATP concentration. The error bars represent the standard deviation of three independent measurements



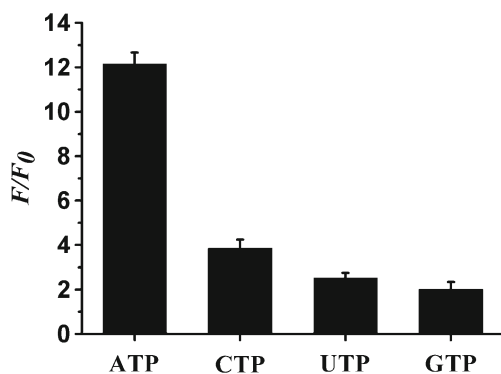


**Fig. 5** Selectivity of ATP.  $F_0$  and  $F$  are fluorescence intensity of DNA-Ag NCs before and after the addition of ATP, CTP, UTP, or GTP, respectively. The error bars represent the standard deviation of three independent measurements

can be attributed to Ag (0) in the BT5T5-Cu/Ag NCs [38, 39]. There are two peaks in the expanded spectrum of Cu 2p (Fig. 3c); the binding energy peak at 932.7 eV for Cu 2p<sub>3/2</sub> suggests the presence of Cu (I) and/or Cu (0) in the BT5T5-Cu/Ag NCs [40, 41]. Cu<sup>+</sup> and Cu<sup>0</sup> species can not be differentiated by Cu 2p<sub>3/2</sub> XPS as they are separated by only 0.1 eV [41]. The peak at 952.5 eV corresponds to the literature value of 952.2 eV (Cu 2p<sub>1/2</sub>) [40, 42], which presumes the presence of elemental Cu (0) in BT5T5-Cu/Ag NCs.

## Optimization of experimental conditions for ATP determination

### Response of different DNA-Cu/Ag NCs to ATP

According to the illustration in Scheme 1, the addition of ATP changes the conformation of the aptamer, bringing the two darkish Cu/Ag NCs into close proximity and resulting in enhanced fluorescence. As shown in ESM Fig. S6, as expected, the fluorescence intensities of eight DNA-Cu/Ag NCs increase upon the addition of ATP, and the relative intensity of the BT5T5-Cu/Ag NCs ( $F/F_0$ , and  $F_0$  and  $F$  are the fluorescence intensities of NCs alone and with 10 mM ATP, respectively) is the largest among them. Thus, the BT5T5-Cu/Ag

NCs are more sensitive and are chosen as the ATP probe to perform the following experiments.

### Optimization of pH

The variation in the fluorescence of BT5T5-Cu/Ag NCs with pH value was further investigated. ESM Fig. S7 demonstrates that the  $F/F_0$  values of BT5T5-Cu/Ag NCs gradually increase from pH 5.0 to 7.0 and then decrease from pH 7.0 to 9.0; therefore, the optimal pH is 7.0 for the BT5T5-Cu/Ag NCs sensing system.

### Determination of incubation time for BT5T5-Cu/Ag NCs with ATP

The incubation time for BT5T5-Cu/Ag NCs and ATP was investigated. ESM Fig. S8 (see) shows that the fluorescence of BT5T5-Cu/Ag NCs gradually increases with the increasing incubation time, reaching a plateau at 5 min, and then remaining almost constant for at least 2 h, so 5 min is regarded as the optimal examination time for ATP.

### Detection of ATP

Quantitative detection of ATP using a BT5T5-Cu/Ag NCs sensing system was performed under the optimal experimental conditions. After ATP (0–22 mM) was added to the solution of BT5T5-Cu/Ag NCs (see Section detection of ATP and ADA), the fluorescence emission was determined. As shown in Fig. 4a and b, the fluorescence of BT5T5-Cu/Ag NCs gradually increases with the addition of ATP within the range of 2–18 mM ( $R = 0.9975$ , the linear regression equation is  $F = -111.6 + 328.2C_{ATP}$ ), and the limit of detection (LOD) of 7.0  $\mu$ M was calculated based on  $3\sigma_0/k$  ( $\sigma_0$  is calculated by the standard deviation of the background, and the slope of calibration line is  $k$ ). As shown in ESM Table S2, this LOD is far lower than those of the previously reported fluorescence sensors for ATP detection [36, 43–45]; therefore, the proposed method is highly sensitive.

**Fig. 6** (a) Fluorescence spectra ( $\lambda_{ex} = 460$  nm) of BT5T5-Cu/Ag NCs with the addition of 10 mM ATP with ADA in different concentrations. (b) Change in fluorescence intensity at 550 nm as a function of ADA concentration. The error bars represent the standard deviation of three independent measurements

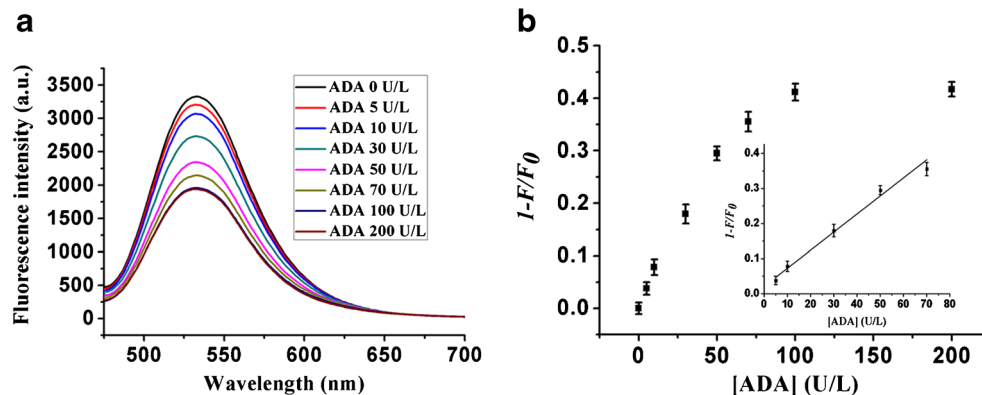


**Table 1** The concentration of ATP in fetal bovine serum solution measured with the proposed method ( $N=3$ )

Samples	Spiked (mM)	Measured (mM) mean <sup>a</sup> ± SD <sup>b</sup>	Recovery (%)	RSD (%)
1	5	5.2 ± 0.12	104.0	2.31
2	10	10.4 ± 0.05	104.0	0.48
3	15	14.9 ± 0.11	99.3	0.74
4	17	17.4 ± 0.22	102.4	1.26

<sup>a</sup> The mean of three determinations<sup>b</sup> SD = standard deviation

In addition, ATP was detected using a BT5T5-Ag NC sensing system. ESM Fig. S9a and b demonstrate that the fluorescence intensity of BT5T5-Ag NCs is enhanced with an increase in ATP from 6 to 16 mM ( $R=0.9822$ ). The linear regression equation is  $F = -425.3 + 468.6C_{ATP}$ , and the LOD is 498  $\mu$ M. This LOD is 70 times that of BT5T5-Cu/Ag NCs, and there is a narrow liner range. Thus, BT5T5-Cu/Ag NCs possess a greater capability to detect ATP.

The fluorescence lifetime at 540 nm for BT5T5-Cu/Ag NCs alone and with ATP was also investigated (ESM Fig. S10). As shown in ESM Table S3, the fluorescence transient of BT5T5-Cu/Ag NCs presents a tri-exponential time constant, which illustrates that the average fluorescence lifetime of BT5T5-Cu/Ag NCs fails to change in the presence of ATP, demonstrating that the interaction of ATP with NCs is a static process.

### Selectivity of the DNA-Cu/Ag NCs toward ATP

Selectivity is a key parameter in assessing the performance of fluorescent probes. To evaluate the specificity of the proposed strategy using BT5T5-Cu/Ag NCs for ATP detection, ATP and other analogues including CTP, UTP, and GTP were investigated. Figure 5 shows that only the target ATP causes an obvious increase in  $F/F_0$ . The results clearly reveal high specificity of the proposed strategy towards ATP.

### Detection of ADA

Firstly, the incubation time of ATP with ADA was investigated. A mixture of 10 mM ATP and 10 U/L ADA incubated at different times was added to BT5T5-Cu/Ag NCs. ESM Fig. S11 shows that the fluorescence of BT5T5-Cu/Ag NCs decreases from 0 to 0.5 h and reaches a plateau after 0.5 h. Thus, the optimal incubation time of ATP with ADA is 0.5 h.

Next, different concentrations of ADA (0–200 U/L) were pre-incubated with 10 mM ATP for 0.5 h, and the mixed solution was separately added to BT5T5-Cu/Ag NCs. After incubation for 5 min, the fluorescence spectrum of each sample was measured (Fig. 6a). As shown in Fig. 6b, the relative fluorescence intensity ( $I-F/F_0$ ) is gradually enhanced with the

addition of ADA within the range of 5–70 U/L ( $R=0.9918$ , the linear regression equation is  $I-F/F_0 = 0.0209 + 0.0051C_{ADA}$ ), and ADA is detected as low as 5 U/L in the linear range from 5 to 50 U/L. Therefore, the BT5T5-Cu/Ag NCs/ATP system is further developed as an ADA-sensing system.

### Detection of ATP and ADA in real samples

In order to evaluate the application and accuracy of the proposed sensing system in the real sample, 5, 10, 15, or 17 mM ATP was separately added to 100-fold-diluted fetal bovine serum and determined by the proposed method, and the recoveries and the relative standard deviations (RSD) are summarized in Table 1. It is found that the recoveries vary within the range of 99.3–104.0%, with RSD of 0.48–2.31%, which indicates that the proposed method has high precision. The current results are also comparable with the reported values [46, 47], demonstrating that the proposed strategy is reliable for ATP assay in real samples. In addition, the recoveries of ADA vary from 99.5% to 104.0% in the diluted fetal bovine serum, with RSD of less than 2.50% (ESM Table S4), which shows that the proposed method is also practicable for ADA assay.

RSD = relative standard deviation.

### Conclusions

In conclusion, a turn-on fluorescent probe for ATP detection was developed using BT5T5-stabilized Cu/Ag NCs. This probe shows good sensitivity and specificity to ATP, and the detection procedure is simple and rapid. The sensing method is also applied to detect ATP in real samples. Therefore, this sensor holds potential for application in the fields of biochemical research and clinical diagnostics. Although ADA can also be monitored by the BT5T5-Cu/Ag NCs/ATP system, it is a signal-off detection and needs a longer incubation time. Thus, a rapid turn-on detection probe for ADA needs to be developed in the future.

**Acknowledgments** This work was supported by the National Natural Science Foundation of China (21171108).

## Compliance with ethical standards

**Conflict of interest** The authors declare that they have no competing interests.

## References

- Park KS, Oh SS, Soh HT, Park HG. Target-controlled formation of silver nanoclusters in abasic site-incorporated duplex DNA for label-free fluorescence detection of theophylline. *Nanoscale*. 2014;6:9977–82.
- Park KS, Park HG. A DNA-templated silver nanocluster probe for label-free, turn-on fluorescence-based screening of homo-adenine binding molecules. *Biosens Bioelectron*. 2015;64:618–24.
- Zhang L, Liang R-P, Xiao S-J, Bai J-M, Zheng L-L, Zhan L, et al. DNA-templated Ag nanoclusters as fluorescent probes for sensing and intracellular imaging of hydroxyl radicals. *Talanta*. 2014;118:339–47.
- Choi S, Dickson RM, Yu J. Developing luminescent silver nanodots for biological applications. *Chem Soc Rev*. 2012;41:1867–91.
- Guo W, Yuan J, Dong Q, Wang E. Highly sequence-dependent formation of fluorescent silver nanoclusters in hybridized DNA duplexes for single nucleotide mutation identification. *J Am Chem Soc*. 2010;132:932–4.
- MacLean JL, Morishita K, Liu J. DNA stabilized silver nanoclusters for ratiometric and visual detection of Hg<sup>2+</sup> and its immobilization in hydrogels. *Biosens Bioelectron*. 2013;48:82–6.
- Shang L, Dong S, Nienhaus GU. Ultra-small fluorescent metal nanoclusters: synthesis and biological applications. *Nano Today*. 2011;6:401–18.
- Yin J, He X, Wang K, Qing Z, Wu X, Shi H, et al. One-step engineering of silver nanoclusters-aptamer assemblies as luminescent labels to target tumor cells. *Nanoscale*. 2012;4:110–2.
- Zhou Z, Du Y, Dong S. DNA-Ag nanoclusters as fluorescence probe for turn-on aptamer sensor of small molecules. *Biosens Bioelectron*. 2011;28:33–7.
- Diez I, Kanyuk MI, Demchenko AP, Walther A, Jiang H, Ikkala O, et al. Blue, green and red emissive silver nanoclusters formed in organic solvents. *Nanoscale*. 2012;4:4434–7.
- Enkin N, Sharon E, Golub E, Willner I. Ag Nanocluster/DNA hybrids: functional modules for the detection of nitroaromatic and RDX explosives. *Nano Lett*. 2014;14:4918–22.
- Park KS, Park HG. Technological applications arising from the interactions of DNA bases with metal ions. *Curr Opin Biotechnol*. 2014;28:17–24.
- Richards CI, Choi S, Hsiang J-C, Antoku Y, Vosch T, Bongiorno A, et al. Oligonucleotide-stabilized Ag nanocluster fluorophores. *J Am Chem Soc*. 2008;130:5038–9.
- Gwinn EG, O'Neill P, Guerrero AJ, Bouwmeester D, Fygenon DK. Sequence-dependent fluorescence of DNA-hosted silver nanoclusters. *Adv Mater*. 2008;20:279–83.
- Li J, Zhong X, Zhang H, Le XC, Zhu J-J. Binding-induced fluorescence turn-on assay using aptamer-functionalized silver Nanocluster DNA probes. *Anal Chem*. 2012;84:5170–4.
- Qian Y, Zhang Y, Lu L, Cai Y. A label-free DNA-templated silver nanocluster probe for fluorescence on-off detection of endonuclease activity and inhibition. *Biosens Bioelectron*. 2014;51:408–12.
- Yeh H-C, Sharma J, Han JJ, Martinez JS, Werner JH. A DNA-silver nanocluster probe that fluoresces upon hybridization. *Nano Lett*. 2010;10:3106–10.
- Chen W-Y, Lan G-Y, Chang H-T. Use of fluorescent DNA-templated gold/silver Nanoclusters for the detection of sulfide ions. *Anal Chem*. 2011;83:9450–5.
- Su Y-T, Lan G-Y, Chen W-Y, Chang H-T. Detection of copper ions through recovery of the fluorescence of DNA-templated copper/silver nanoclusters in the presence of mercaptopropionic acid. *Anal Chem*. 2010;82:8566–72.
- Gessi S, Cattabriga E, Avitabile A, Gafa R, Lanza G, Cavazzini L, et al. Elevated expression of A(3) adenosine receptors in human colorectal cancer is reflected in peripheral blood cells. *Clin Cancer Res*. 2004;10:5895–901.
- Stagg J, Smyth MJ. Extracellular adenosine triphosphate and adenosine in cancer. *Oncogene*. 2010;29:5346–58.
- Spychala J. Tumor-promoting functions of adenosine. *Pharmacol Ther*. 2000;87:161–73.
- Yan X, Cao Z, Kai M, Lu J. Label-free aptamer-based chemiluminescence detection of adenosine. *Talanta*. 2009;79:383–7.
- Yang J, Xu GW, Kong HW, Zheng WF, Pang T, Yang Q. Artificial neural network classification based on high-performance liquid chromatography of urinary and serum nucleosides for the clinical diagnosis of cancer. *J Chromatogr B Anal Technol Biomed Life Sci*. 2002;780:27–33.
- Siragy HM, Linden J. Sodium intake markedly alters renal interstitial fluid adenosine. *Hypertension*. 1996;27:404–7.
- Tzeng H-F, Hung C-H, Wang J-Y, Chou C-H, Hung H-P. Simultaneous determination of adenosine and its metabolites by capillary electrophoresis as a rapid monitoring tool for 5'-nucleotidase activity. *J Chromatogr A*. 2006;1129:149–52.
- Sottofattori E, Anzaldi M, Ottonello L. HPLC determination of adenosine in human synovial fluid. *J Pharm Biomed Anal*. 2001;24:1143–6.
- Xiang Y, Tong A, Lu Y. Abasic site-containing DNAzyme and aptamer for label-free fluorescent detection of Pb<sup>2+</sup> and adenosine with high sensitivity, selectivity, and tunable dynamic range. *J Am Chem Soc*. 2009;131:15352–7.
- Chen J-W, Liu X-P, Feng K-J, Liang Y, Jiang J-H, Shen G-L, et al. Detection of adenosine using surface-enhanced Raman scattering based on structure-switching signaling aptamer. *Biosens Bioelectron*. 2008;24:66–71.
- Zhu X, Zhang Y, Yang W, Liu Q, Lin Z, Qiu B, et al. Highly sensitive electrochemiluminescent biosensor for adenosine based on structure-switching of aptamer. *Anal Chim Acta*. 2011;684:121–5.
- Yin B-C, Ma J-L, Le H-N, Wang S, Xu Z, Ye B-C. A new mode to light up an adjacent DNA-scaffolded silver probe pair and its application for specific DNA detection. *Chem Commun*. 2014;50(100):15991–4.
- Aldrich MB, Blackburn MR, Kellems RE. The importance of adenosine deaminase for lymphocyte development and function. *Biochem Biophys Res Commun*. 2000;272:311–5.
- Loo K, Degtyareva N, Park J, Sengupta B, Reddish M, Rogers CC, et al. Ag<sup>+</sup>-mediated assembly of 5'-guanosine monophosphate. *J Phys Chem B*. 2010;114:4320–6.
- Liu X, Hu R, Gao Z, Shao N. Photoluminescence mechanism of DNA-templated silver nanoclusters: coupling between surface plasmon and emitter and sensing of lysozyme. *Langmuir*. 2015;31:5859–67.
- Shaviv E, Schubert O, Alves-Santos M, Goldoni G, Di Felice R, Vallee F, et al. Absorption properties of metal-semiconductor hybrid nanoparticles. *ACS Nano*. 2011;5:4712–9.
- Xu J, Wei C. The aptamer DNA-templated fluorescence silver nanoclusters: ATP detection and preliminary mechanism investigation. *Biosens Bioelectron*. 2017;87:422–7.
- Song X-R, Goswami N, Yang H-H, Xie J. Functionalization of metal nanoclusters for biomedical applications. *Analyst*. 2016;141:3126–40.

38. Krishnadas KR, Ghosh A, Baksi A, Chakraborty I, Natarajan G, Pradeep T. Intercluster reactions between  $\text{Au-25(SR)(18)}$  and  $\text{Ag-44(SR)(30)}$ . *J Am Chem Soc.* 2016;138:140–8.
39. Zhou Q, Lin Y, Xu M, Gao Z, Yang H, Tang D. Facile synthesis of enhanced fluorescent gold-silver bimetallic nanocluster and its application for highly sensitive detection of inorganic pyrophosphatase activity. *Anal Chem.* 2016;88:8886–92.
40. Platzman I, Brener R, Haick H, Tannenbaum R. Oxidation of polycrystalline copper thin films at ambient conditions. *J Phys Chem C.* 2008;112:1101–8.
41. Deutsch KL, Shanks BH. Active species of copper chromite catalyst in C-O hydrogenolysis of 5-methylfurfuryl alcohol. *J Catal.* 2012;285:235–41.
42. Liu P, Hensen EJ. Highly efficient and robust  $\text{Au/MgCuCr}_2\text{O}_4$  catalyst for gas-phase oxidation of ethanol to acetaldehyde. *J Am Chem Soc.* 2013;135:14032–5.
43. Liao D, Jiao H, Wang B, Lin Q, Yu C. KF polymerase-based fluorescence aptasensor for the label-free adenosine detection. *Analyst.* 2012;137:978–82.
44. Lu L, Qian Y, Wang L, Ma K, Zhang Y. Metal-enhanced fluorescence-based core-shell  $\text{Ag@SiO}_2$  nanoflakes for affinity biosensing via target-induced structure switching of aptamer. *ACS Appl Mater Interfaces.* 2014;6:1944–50.
45. Ma J-L, Yin B-C, Ye B-C. A versatile proximity-dependent probe based on light-up DNA-scaffolded silver nanoclusters. *Analyst.* 2016;141:1301–6.
46. Song Q-W, Wang R-H, Sun F-F, Chen H-K, Wang Z-M-K, Na N, et al. A nuclease-assisted label-free aptasensor for fluorescence turn-on detection of ATP based on the in situ formation of copper nanoparticles. *Biosens Bioelectron.* 2017;87:760–3.
47. Zhu Y, Hu X-C, Shi S, Gao R-R, Huang H-L, Zhu Y-Y, et al. Ultrasensitive and universal fluorescent aptasensor for the detection of biomolecules (ATP, adenosine and thrombin) based on DNA/Ag nanoclusters fluorescence light-up system. *Biosens Bioelectron.* 2016;79:205–12.

**Publisher's note** Springer Nature remains neutral with regard to jurisdictional claims in published maps and institutional affiliations.